





# The neural basis for violations of Weber's law in self-motion perception

Jerome Carriot<sup>a</sup>, Kathleen E. Cullen<sup>b,c,d,e</sup> , and Maurice J. Chacron<sup>a,1</sup> 

<sup>a</sup>Department of Physiology, McGill University, Montréal, QC H3G 1Y6, Canada; <sup>b</sup>Department of Biomedical Engineering, Johns Hopkins University, Baltimore, MD 21218; <sup>c</sup>Department of Otolaryngology-Head and Neck Surgery, Johns Hopkins University School of Medicine, Baltimore, MD 21205; <sup>d</sup>Department of Neuroscience, Johns Hopkins University School of Medicine, Baltimore, MD 21205; and <sup>e</sup>Kavli Neuroscience Discovery Institute, Johns Hopkins University, Baltimore, MD 21218

Edited by Marlene Behrmann, Carnegie Mellon University, Pittsburgh, PA, and approved June 25, 2021 (received for review December 4, 2020)

**A prevailing view is that Weber's law constitutes a fundamental principle of perception. This widely accepted psychophysical law states that the minimal change in a given stimulus that can be perceived increases proportionally with amplitude and has been observed across systems and species in hundreds of studies. Importantly, however, Weber's law is actually an oversimplification. Notably, there exist violations of Weber's law that have been consistently observed across sensory modalities. Specifically, perceptual performance is better than that predicted from Weber's law for the higher stimulus amplitudes commonly found in natural sensory stimuli. To date, the neural mechanisms mediating such violations of Weber's law in the form of improved perceptual performance remain unknown. Here, we recorded from vestibular thalamocortical neurons in rhesus monkeys during self-motion stimulation. Strikingly, we found that neural discrimination thresholds initially increased but saturated for higher stimulus amplitudes, thereby causing the improved neural discrimination performance required to explain perception. Theory predicts that stimulus-dependent neural variability and/or response nonlinearities will determine discrimination threshold values. Using computational methods, we thus investigated the mechanisms mediating this improved performance. We found that the structure of neural variability, which initially increased but saturated for higher amplitudes, caused improved discrimination performance rather than response nonlinearities. Taken together, our results reveal the neural basis for violations of Weber's law and further provide insight as to how variability contributes to the adaptive encoding of natural stimuli with continually varying statistics.**

neural coding | vestibular system | Weber's law

**W**eber's law states that the discrimination threshold or "just noticeable difference" (JND) is proportional to stimulus amplitude (1). While the prevailing view is that this law holds across multiple sensory modalities and species (1–6), more recent studies have shown that Weber's law consistently does not hold across sensory modalities when higher amplitude, physiologically relevant stimuli are considered [e.g., auditory (7, 8), visual (9), and vestibular (10–12) systems]. Specifically, discrimination thresholds saturate for higher amplitudes and are thus not proportional to stimulus amplitude across the entire range (7, 9–13). While there is a building consensus that perceptual discrimination performance is better than that predicted from Weber's law across sensory modalities, to date, the neural substrates underlying such violations remain unknown. It is generally thought that a decrease in neural sensitivity or gain with increasing stimulus amplitude provides the neural basis for Weber's law (14–16). Such "Weber adaptation" is advantageous for sensory coding as it serves to broaden the dynamic range and to maintain information capacity in response to stimuli whose amplitudes vary over orders of magnitude (14, 15, 17–21). However, Weber adaptation is not sufficient to explain the violations of Weber's law that have been observed across modalities. Thus, what mechanisms underlie perception across the

entire range of stimuli encountered in the natural environment remains a fundamental and unanswered question.

Here, we took advantage of a sensory system with well-described circuitry to gain insight into how neural response properties give rise to perceptual performance. Specifically, the vestibular system generates vital reflexes that stabilize gaze and posture during movement, and makes a vital contribution to self-motion perception (22–25). Previous studies have demonstrated that vestibular perception violates Weber's law. Specifically, the discrimination performance of human subjects is much better than expected for higher rotational stimulus amplitudes (10–12) commonly experienced during natural everyday activities (e.g., walking) (26). Head motion is initially sensed by peripheral vestibular afferents that make synaptic contact with central vestibular nuclei neurons (27). Neurons within the ventral posterior lateral (VPL) thalamus receive direct input from the vestibular nuclei (28) and project to higher cortical areas (29, 30) that mediate self-motion perception (31) (see ref. 32 for review). Afferents and vestibular nuclei neurons do not display significant nonlinearities in their responses to the low frequency stimuli that have been used in perceptual testing (33–36). In contrast, neurons at the next stage of processing within area VPL have been shown to respond nonlinearly to head motion, notably showing decreases in neural sensitivity with increasing stimulus amplitude (37–41). However, whether such nonlinearities can explain the observed violations of Weber's law remains unknown to date.

## Significance

**An unanswered question is why perceptual performance consistently exceeds that predicted from Weber's law across sensory modalities. Here, we provide a neural basis for such violations of Weber's law. Specifically, we demonstrate that the structure of variability in vestibular thalamocortical neurons gives rise to the improvement in neural discrimination performance required to explain previous perceptual results. Our results not only have important consequences for understanding how sensory pathways generate perception but also provide an unexpected function for neural variability. Moreover, our findings make an important contribution by suggesting that improved perceptual discrimination performance observed across modalities is a signature of optimized coding in the brain when neural variability is taken into account.**

Author contributions: J.C., K.E.C., and M.J.C. designed research; J.C. performed research; J.C. and M.J.C. analyzed data; and J.C., K.E.C., and M.J.C. wrote the paper.

The authors declare no competing interest.

This article is a PNAS Direct Submission.

Published under the PNAS license.

<sup>1</sup>To whom correspondence may be addressed. Email: maurice.chacron@mcgill.ca.

This article contains supporting information online at <https://www.pnas.org/lookup/suppl/doi:10.1073/pnas.2025061118/-DCSupplemental>.

Published September 2, 2021.

Accordingly, we investigated the neural substrate underlying improved discrimination performance for higher amplitude vestibular stimuli. We recorded the activities of vestibular thalamocortical neurons in response to rotational self-motion stimuli with varying amplitude in rhesus monkeys. We found that neural discrimination thresholds were lower than predicted for higher stimulus amplitudes, thereby providing a neural correlate for previous results showing improved perceptual discrimination performance (10). Theory predicts that discrimination thresholds are determined not only by neural gain but also by variability (42). Consequently, we characterized how each quantity varied as a function of stimulus amplitude. We found that the dependence of neural variability on stimulus amplitude accounted for previous perceptual results.

Specifically, variability initially increased but saturated for higher stimulus amplitudes, thereby causing the improved neural discrimination performance required to explain perception. Taken together, our results reveal that amplitude-dependent changes in neural variability can account for the fact that self-motion perceptual performance is better than that predicted from Weber's law. Our findings, furthermore, provide insight as to how variability contributes to the adaptive encoding of natural stimuli with continually varying statistics.

## Results

We recorded the activities of  $n = 28$  neurons within area VPL of the thalamus in three awake-behaving rhesus macaque monkeys (*Macaca mulatta*; 16 from monkey B, 8 from monkey D, and 4 from monkey S), for which we were able to maintain isolation during the highly dynamic self-motion stimuli described in the next paragraph. These neurons were all responsive to sinusoidal whole-body yaw rotations but did not respond to horizontal or vertical eye movements, movement of small objects in the environment, or onset/offset of lights in the room (see *Materials and Methods*). As mentioned above, VPL neurons receive input from vestibular afferents via vestibular nuclei neurons and, in turn, project to higher cortical areas (Fig. 1A).

**VPL Neurons Display Decreased Gain and Increased Variability to Increases in Stimulus Amplitude.** The goal of our study was to understand the neural basis as to why vestibular perceptual performance is better than that predicted from Weber's law (10–12). Specifically, we focused on why perceptual discrimination performance was much better than predicted for higher stimulus amplitudes. Because discrimination performance is strongly impacted by neural sensitivity or gain, we first investigated how neural gain varied as a function of stimulus amplitude (see *Materials and Methods*). Our stimuli consisted of sinusoidal whole-body rotations whose amplitude increased linearly with time (i.e., ramps; Fig. 1B, *Top Left*). We found that vestibular thalamocortical neurons responded to ramp stimuli through sinusoidal modulations in firing rate (Fig. 1B, *Bottom Left*) but that the firing rate modulation increased more slowly than that of the ramp stimulus (Fig. 1B, *Right*, compare blue and red). Specifically, the depth of the firing rate modulation initially increased but then appeared for the most part invariant at higher stimulus amplitudes. This indicates a decrease in neural gain with increasing stimulus amplitude.

To better understand the dependency of gain on stimulus amplitude, we plotted the firing rate as a function of the head velocity for example low (Fig. 1C) and high (Fig. 1D) stimulus amplitudes. Overall, there was a mostly linear relationship between firing rate and head velocity in both cases (compare Fig. 1C and D). However, the slope of the best-fit straight line to the data (i.e., neural gain) was lower for the example high amplitude stimuli (compare blue and red lines in Fig. 1D). Overall, we found that the gain of vestibular thalamocortical neurons strongly decreased with increasing stimulus amplitude (Fig. 1E). Such

nonlinearities are consistent with previous results (37, 40). Interestingly, we further found that the inverse gain increased linearly with increasing stimulus amplitude (Fig. 1E, *Inset*), implying that vestibular thalamocortical neurons display “Weber adaptation” or “Weber–Fechner gain scaling,” as seen in other systems (14–16). We note that, while the mechanisms that mediate contrast gain scaling in vestibular thalamocortical neurons remain unknown, previous studies carried out in other systems have reported that the time course of such an adaptation can be as low as 100 ms (43). We predict that adaptation occurs essentially instantaneously when compared with the timescale of the slowly time-varying stimuli used in the current study. Furthermore, we note that other features of the head-motion stimulus (e.g., acceleration) increase with increasing amplitude and thus could be used to calibrate contrast gain scaling observed here relative to velocity.

However, it is important to emphasize that, theoretically, discriminability will be determined by variability as well as gain (42). On the one hand, if variability does not vary as a function of stimulus amplitude, then variations in discriminability with stimulus amplitude can only be attributed to changes in neural gain. On the other hand, variability that is dependent on stimulus amplitude can contribute to determining how discriminability will vary with amplitude and thus potentially explain why discrimination performance is better than that predicted from Weber's law. Accordingly, we next characterized the dependency of neural variability on stimulus amplitude (see *Materials and Methods*). Our results show that the neural variability of vestibular thalamocortical neurons strongly varied with increasing stimulus amplitude (Fig. 1F). Specifically, neural variability initially increased for low amplitudes (i.e.,  $<45$  deg/s) but saturated if not slightly decreased for high amplitudes (i.e.,  $>45$  deg/s; Fig. 1F). This latter saturation is most likely because of the fact that the neural response was for the most part invariant for these stimulus amplitudes. Thus, both variability and gain strongly varied with stimulus amplitude for vestibular thalamocortical neurons.

**The Combined Effects of Gain and Variability Provide a Neural Correlate for Vestibular Perception.** So far, our results showed that both gain and variability must be taken into account when quantifying discriminability. Accordingly, we next explicitly assessed whether these factors could explain why vestibular perceptual performance is better than that predicted from Weber's law (10). To do so, we computed neural discrimination thresholds for our dataset by quantifying the ability of an ideal observer to discriminate between different stimulus amplitudes based on changes in firing rate. The methodology is illustrated in Fig. 2A–C (see *Materials and Methods*). Specifically, for each head velocity, the firing rate distribution was computed and the discriminability between distributions obtained at different head velocities was computed using the  $d'$  measure (Fig. 2A–C; see *Materials and Methods*). The discrimination threshold then corresponds to the minimum change in stimulus amplitude that gives rise to firing rate distributions that are discriminable from each other, as quantified by a value of  $d' = 1.16$  (Fig. 2C).

Intuitively, discrimination thresholds should increase with decreasing gain because the firing rate distributions will only become discriminable from one another if there is a larger change in stimulus amplitude, as illustrated in Fig. 2A–C. However, increased variability will also lead to increased discrimination threshold because the firing rate distributions will then only become discriminable from one another if there is a larger change in stimulus amplitude. Overall, we found that the stimulus amplitude-dependent gain and variability of vestibular thalamocortical neurons led to discrimination thresholds that were not proportional to stimulus amplitude over the entire range (Fig. 2D). Indeed, while discrimination thresholds increased linearly at low (i.e.,  $<\sim 50$  deg/s), they increased at a lower rate at higher (i.e.,  $>\sim 50$  deg/s) amplitudes. To quantify this change, we fitted straight lines to the

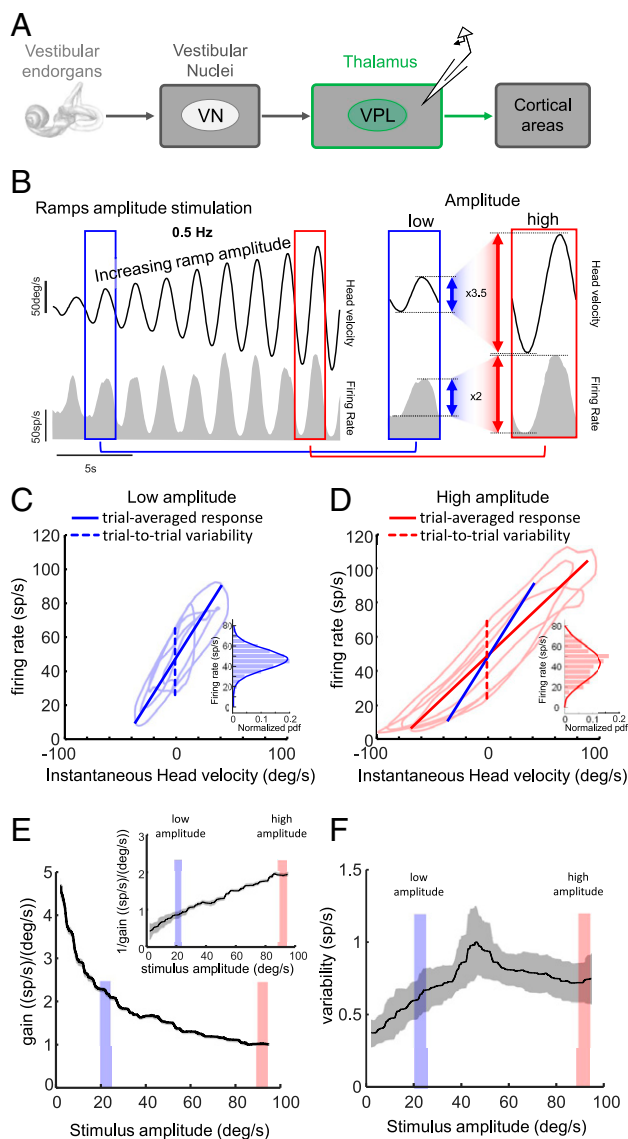


**Fig. 1.** (A) Schematic showing the organization of early and central vestibular pathways. Vestibular afferents emanate from the vestibular endorgans (*Left*) and project to the vestibular nuclei (VN, *Center Left*). VN neurons project to the ventroposterior-lateral (VPL) area of the thalamus (*Center*), from which recordings were made. These, in turn, project to cortical areas (*Center Right*), thereby giving rise to self-motion perception (*Right*). (B) Stimuli used in this study consisted of sinusoidal yaw rotations whose amplitude increased linearly with time (i.e., ramp; *Top Left*). The bottom left shows the time-dependent firing rate (gray) of a typical VPL neuron in response to the stimulus shown on top. It is seen that the firing rate modulation does not increase as fast as the stimulus amplitude. The right panels show portions of the stimulus and response for low (blue) and high (red) amplitudes. While the stimulus amplitude increases by 3.5, the corresponding firing rate modulation only increased by 2 (see blue and red arrows), indicating that neural gain (i.e., the ratio of firing rate modulation to stimulus amplitude) decreases. (C) Firing rate as a function of head velocity for low amplitudes (light blue), showing the trial-averaged response (blue line) as well as trial-to-trial variability (dashed blue line). (*Inset*) The firing rate distribution for zero instantaneous head velocity was not significantly different from normal ( $P = 0.08$ ; Lilliefors test). The solid line shows the Gaussian fit. (D) Same as C but for high stimulus amplitudes. Note the decrease in the slope of the trial-averaged response, which is the gain. We further note that, while there was rectification for large amplitude negative head velocities, we did not observe saturation for large positive head velocities. (*Inset*) The firing rate distribution for zero instantaneous head velocity was not significantly different from normal ( $P = 0.45$ ; Lilliefors test). The solid line shows the Gaussian fit. (E) Population-averaged neural gain as

low (0 to 25 deg/s) and high (75 to 100 deg/s) portions of the curve and computed the relative change in slope, as well as the value of the stimulus amplitude at which both lines intersect (i.e., the transition amplitude; see *Materials and Methods*). We found similar results when systematically varying the frequency of the sinusoidal ramp within the natural range (*SI Appendix, Fig. S1*). As such, both the relative change in slope (Fig. 2 *E, Top*) and the transition amplitude (Fig. 2 *E, Bottom*) were independent of the sinusoidal ramp frequency used. This indicates that our results are robust.

To summarize, Fig. 2 *D* and *E* demonstrate that neural discrimination thresholds tend to saturate for higher stimulus amplitudes, which is a trend comparable to that previously observed for perception (10). Accordingly, we next explicitly addressed our central question of whether neural discrimination thresholds can explain previously observed violations of Weber's law. For single neurons, we found a qualitative match between neural and perceptual discrimination threshold values for all amplitudes tested (Fig. 3 *A, Left*, compare solid magenta and black curves). Indeed, both neural and perceptual discrimination thresholds initially increased linearly at low (i.e.,  $< \sim 50$  deg/s) but saturated at high (i.e.,  $> \sim 50$  deg/s) stimulus amplitudes (Fig. 3 *A*, compare solid magenta and black solid curves to dashed lines). Although neural thresholds were approximately threefold higher than perceptual values, both curves increased linearly at low (i.e.,  $< \sim 50$  deg/s) amplitudes and saturated at high (i.e.,  $> \sim 50$  deg/s) stimulus amplitudes (Fig. 3 *A, Left*, compare magenta and black curves with magenta and black dashed straight lines, respectively). Thus, both neural and perceptual thresholds displayed similar changes in slope (Fig. 3 *A, Middle*), as well as transition amplitudes (Fig. 3 *A, Right*). Importantly, the difference between neural and perceptual threshold values was more or less constant for all stimulus amplitudes (Fig. 3 *A, Left*, compare solid magenta and black curves), suggesting that perception is achieved by integrating the activities of multiple, vestibular thalamocortical neurons.

Finally, to test this hypothesis and, importantly, to quantify the actual number of neurons necessary to achieve perceptual performance, we computed discrimination thresholds from the pooled activities of multiple, vestibular thalamocortical neurons (Fig. 3 *B, Left*; see *Materials and Methods*). As expected, pooling the activities of more neurons (i.e., increasing population size) led to improved discriminability (i.e., a decrease in discrimination threshold; Fig. 3 *B, Middle and Right*). Interestingly, we found that discrimination thresholds computed from the pooled activities of  $n = 12$  neurons reached those reported for perception in the case of both the low and high example stimulus amplitudes (Fig. 3 *B, Middle and Right*). Overall, increasing population size  $n$  from 1 to 12 led to a progressive decrease in neural discrimination thresholds across the entire amplitude range (Fig. 3 *C*). Importantly, discrimination thresholds computed from the pooled activities of  $n = 12$  neurons reached those reported for perception for all amplitudes tested (Fig. 3 *C*, compare black and turquoise curves).

## Discussion

**Summary of Results.** Here, we investigated the mechanisms that underlie the perception of self-motion. Specifically, we tested whether the responses of vestibular thalamocortical neurons can

a function of stimulus amplitude. (*Inset*) The reciprocal of gain increases linearly with increasing stimulus amplitude. The low and high amplitude portions are shown as blue and red bands, respectively. The gray bands show one SEM throughout. The data were well fit by a straight line ( $R^2 = 0.82$ ). (F) Neural variability as a function of stimulus amplitude. The low and high amplitude portions are shown as blue and red bands, respectively. The gray bands show one SEM throughout.

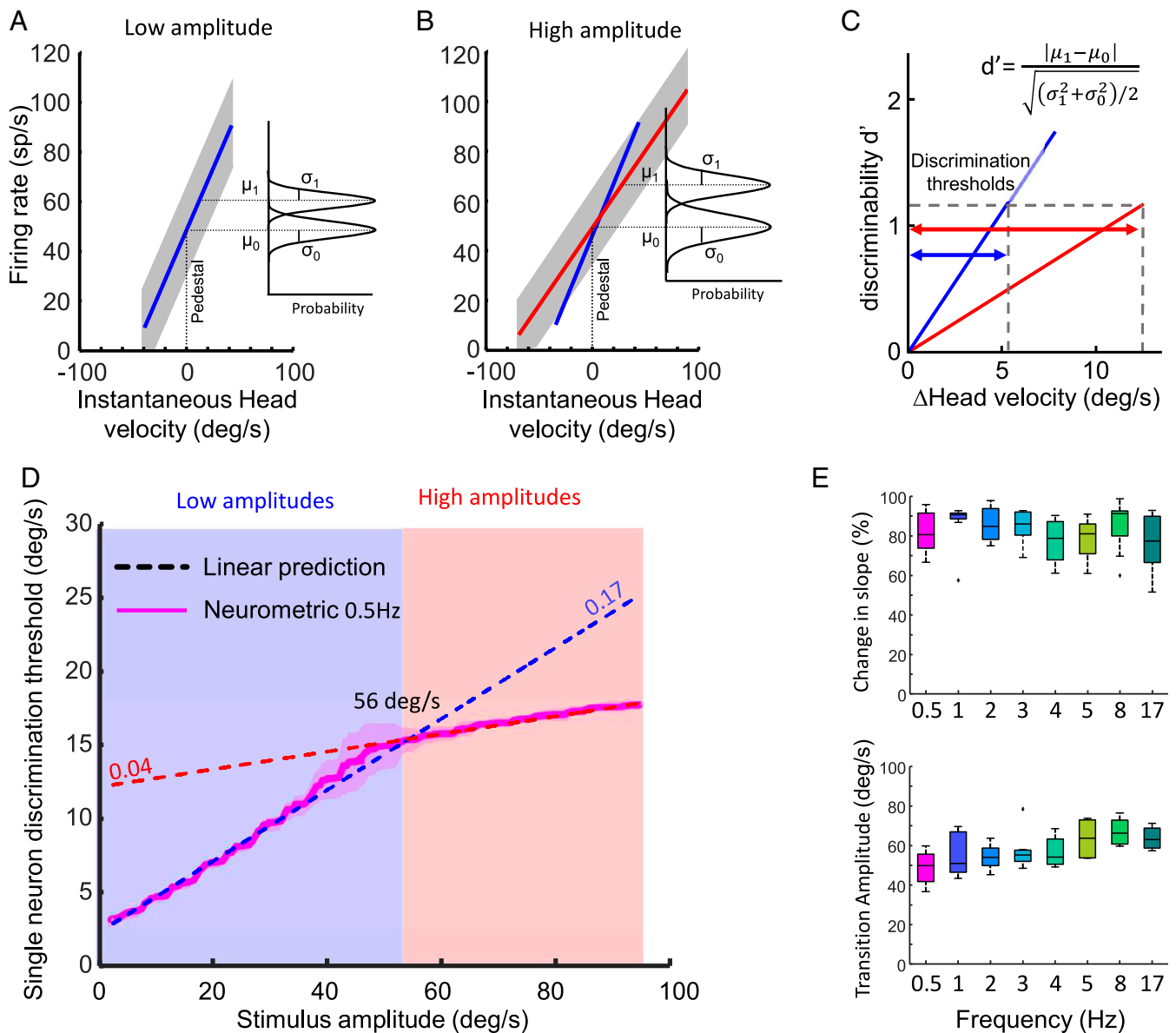


**Fig. 2.** (A) Schematic showing the firing rate as a function of head velocity for low stimulus amplitudes with trial-averaged response shown in blue and the variability shown in gray. For a given head velocity, there is a distribution of firing rates that is approximately normal. (*Inset*) Two example distributions with means  $\mu_0$  and  $\mu_1$  and SDs  $\sigma_0$  and  $\sigma_1$ . We took the pedestal (i.e., reference) to be at 0 deg/s. (B) Same as A but for high stimulus amplitudes. Because the rate at which the firing rate changes with increasing head velocity decreases (black arrow), a greater change in head velocity is required in order to give rise to a given separation between the two distributions. (C) Discriminability between distributions  $d'$  as a function of the change in head velocity for low (blue) and high (red) stimulus amplitudes. It is seen that, for high stimulus amplitudes,  $d'$  increases more slowly than for low-stimulus amplitudes. Consequently, the discrimination threshold, which is the change in head velocity required to give rise to a value of  $d' = 1.16$  (which corresponds to a probability of correct detection of 79.4%), will be greater for high stimulus amplitudes (compare red and blue horizontal arrows). (D) Population-averaged discrimination thresholds for VPL neurons as a function of stimulus amplitude for a 0.5-Hz ramp stimulus. It is seen that the discrimination threshold increases at a higher rate for low (i.e.,  $< \sim 50$  deg/s) and at a lower rate for high (i.e.,  $> \sim 50$  deg/s) stimulus amplitudes (blue vs. red box). Thus, neural discrimination thresholds did not increase linearly with stimulus amplitude (dashed blue line). (E, *Top*) Population-averaged values of the relative change in slope for all frequencies tested. We did not observe significant differences ( $P > 0.15$ , one-way ANOVA). (*Bottom*) Population-averaged values of the transition amplitude for all frequencies tested. We did not observe significant differences ( $P > 0.16$ , except for 0.5 and 17 Hz,  $P > 0.04$ , one-way ANOVA).

account for a violation of Weber's law, namely that discrimination performance is enhanced at higher stimulus amplitudes (10). To do so, we quantified how neural gain and variability varied as a function of stimulus amplitude and computed neural discrimination thresholds. While neural gain strongly decreased as a function of stimulus amplitude, neural variability instead initially increased at low values but saturated at high values. As a result, neural thresholds, contrary to predictions from Weber's law, were not proportional to stimulus amplitude, as they also saturated

at higher values. Furthermore, while single-neuron discrimination thresholds were threefold higher than those of perception, values computed from neural populations agreed with perception for all amplitudes. Thus, overall, the dependency of neural population discrimination thresholds on stimulus amplitude can explain why vestibular perceptual performance is better than that predicted from Weber's law. Taken together, our results uncover a role for neural variability in shaping how sensory pathways generate perception.

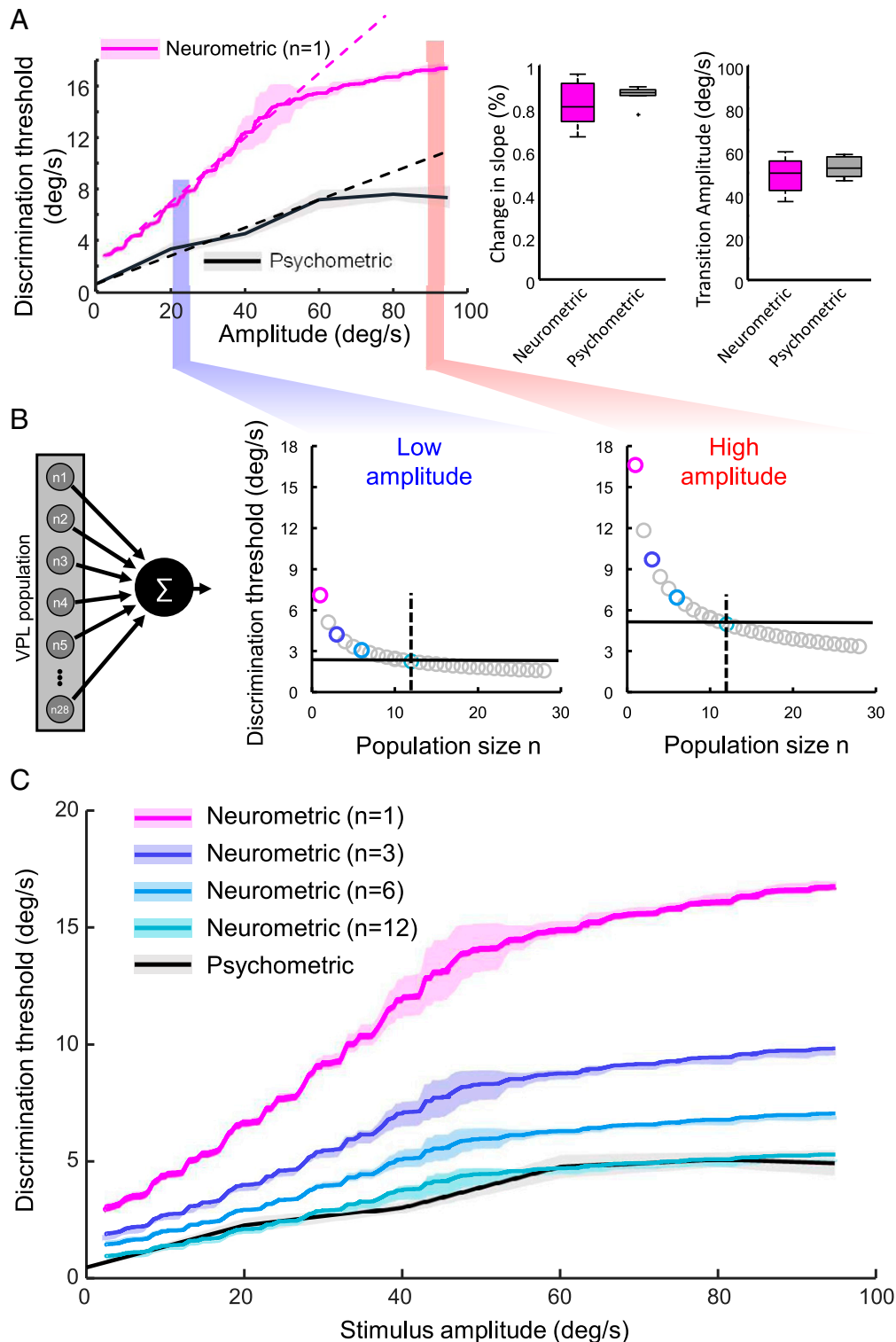


**Fig. 3.** (A, Left) Comparison between vestibular thalamocortical discrimination thresholds at 0.5 Hz (magenta) and perceptual values also at 0.5 Hz (black) as a function of stimulus amplitude. In both cases, discrimination thresholds increase at a higher rate for low (i.e.,  $<50$  deg/s) than for high (i.e.,  $>50$  deg/s) stimulus amplitude, causing a deviation from linearity (compare solid curves and dashed lines). (Middle) Relative changes in slope for neurometric (magenta) and for perception (black) were not significantly different from one another ( $P = 0.91$ , one-way ANOVA). (Right) Transition amplitudes for neurometric (magenta) and for perception (black) were not significantly different from one another ( $P = 0.31$ , one-way ANOVA). (B, Left) Schematic showing a downstream decoder performing a linear sum of input neural activities. (Middle) Discrimination threshold as a function of population size  $n$  for a low stimulus amplitude of 20 to 25 deg/s. (Right) Same as middle panel but for a high stimulus amplitude of 89 to 94 deg/s. In the middle and right panels, the perceptual value is shown as a horizontal black line. (C) Neural discrimination thresholds as a function of stimulus amplitude for population sizes of 1 (magenta), 3 (dark blue), 6 (blue), and 10 (cyan). Also shown is the perceptual data (black). The bands show one SEM throughout. Perceptual data obtained in human subjects is replotted from ref. 10.

### Mechanisms by which Neural Variability Varies with Stimulus Amplitude in Vestibular Thalamocortical Neurons and Implications.

In the current study, we observed that neural variability strongly depended on stimulus amplitude for vestibular thalamocortical neurons. Specifically, we showed that neural variability initially increased linearly for low amplitudes but instead saturated for higher values. This raises the important question as to why have variability at all? For example, one might argue that, if neural variability were to be reduced, then neural discrimination thresholds would be lower, which would then presumably lead to increased perceptual discrimination performance. Neural variability has been observed ubiquitously across systems and species and it remains to be determined whether such variability is beneficial or detrimental to neural coding (44, 45). Specifically, variability could be an unavoidable by-product of the brain's circuitry or, alternatively, might be useful to enhance coding by enabling the brain to better adapt to changing environments.

A second question that is raised by our present results is what mechanisms underlie the saturation of variability observed for high amplitude stimulation? Notably, at the frequency for which we compare our results to psychometric data (i.e., 0.5 Hz), afferents and vestibular nuclei neurons do not display significant response nonlinearities (e.g., inhibitory cutoff or saturation) (33–36). Interestingly, we found qualitatively similar results using higher frequency stimuli that would likely elicit significant response nonlinearities in early vestibular pathways. This suggests that mechanisms beyond a nonlinearity inherited from early vestibular pathways mediate the dependency of neural variability on the stimulus amplitude observed here for vestibular thalamocortical neurons. Prior studies in other sensory systems have shown that neural variability is “quenched” (i.e., reduced) at the onset of stimulation across cortical areas and that the magnitude of this reduction increases with neural gain (46, 47), which resembles our results. Several possible explanations have been proposed ranging from stabilizing the network trajectory near the vicinity of an attractor to increased feedback inhibition, both of which will tend to reduce variability (48, 49). Interestingly, network models containing both recurrent excitatory and feedback inhibitory projections predict that variability initially increases with stimulus amplitude before reaching a maximum and then decreasing (48), which is qualitatively similar to our current experimental findings (Fig. 1F). These models propose that the initial increase in variability is due to hidden feedforward and recurrent excitatory connections, thereby amplifying variability for weak inputs, and that saturation and the subsequent decrease for higher inputs is due to the stabilizing effects of inhibitory feedback (48, 50–53). Accordingly, the dependency of neural variability on stimulus amplitude observed here for thalamocortical neurons could be due to changes in the relative balance between feedforward/recurrent connections and inhibitory feedback from cortical areas. Alternatively, the saturation and slight decrease in variability observed for higher stimulus amplitudes could occur because response nonlinearities, such as phase locking, are then more prevalent for vestibular thalamocortical neurons, as has been previously reported for vestibular afferents (35, 54). Further studies are needed to test these predictions.

### Decoding of VPL Neural Activity by Cortex Leading to Perception.

Our results predict that pooling the activities of multiple (~10) thalamocortical neurons will give rise to discrimination thresholds that match perception. VPL neurons project to cortical areas such as the parietoinsular vestibular cortex, the ventral intraparietal area, area 2v of the intraparietal sulcus, and area 3a in the sulcus centralis (22, 55, 56). Notably, previous work has shown that, consistent with anatomical results, neurons in these cortical areas respond to head motion in darkness. While to date the discrimination thresholds of vestibular, sensitive cortical neurons targeted by VPL to dynamic, rotational stimuli remain

unknown, we predict that the discrimination performance of single cortical neurons will be better (i.e., discrimination thresholds will be lower) than that of single thalamocortical neurons and, importantly, will also saturate at high amplitude values in a similar fashion to what is observed here in order to give rise to perception. In general, the exact number of thalamocortical neurons required to reach perceptual performance will depend on multiple factors, such as differences between methodologies used to obtain neural firing rates. Thus, the analytical approach used here to obtain the time-dependent firing rate most likely provided a lower bound estimate (57). We emphasize, however, that our main finding, that thalamocortical neural discrimination thresholds saturate for high stimulus amplitudes, will not depend qualitatively on the nature of the analytical approach used to compute them.

The present study investigated neural “discrimination” thresholds in the vestibular system. Previous studies have instead focused on quantifying neural “detection” thresholds in subthalamic structures [dynamic rotations (33, 36) and dynamic translations (57, 58)] and comparing these to perceptual detection thresholds [dynamic rotations (59–61) and dynamic translations (25, 62–66)]. Importantly, detection thresholds measure the lowest stimulus amplitude that can be perceived starting from rest, while discrimination thresholds instead measure the smallest change in the stimulus that can be perceived for a given amplitude. Accordingly, detection thresholds cannot be used to test Weber's law. Moreover, we compared our rotational neural discrimination threshold values, obtained from electrophysiological measurements in monkeys, to perceptual discrimination thresholds, obtained from prior studies using human subjects (10). We note that the structure and statistics of the vestibular input experienced by nonhuman primates during natural self-motion closely resemble those observed in humans (26, 67). Thus, given that sensory systems are thought to be adapted to the structure of natural stimuli such as to optimally encode them (68–71), it is likely that the neural mechanisms underlying self-motion perception are similar in both species (72). We further note that Mallery et al. (10) used a “staircase” approach in order to measure perceptual discrimination thresholds, which requires many trials and is currently not feasible for neurophysiological recordings, as it is not possible to hold neurons while moving the animal for such extensive periods of time. Accordingly, to compute neural discrimination thresholds, we used signal detection theory with a probability of correct detection value of 79.4%, which is equivalent to that used by Mallery et al. (10) and allows for better comparison between both datasets.

### Functional Implications for Violations of Weber's Law for Self-Motion Perception and Other Systems.

Our results reveal the neural basis as to why rotational self-motion perceptual discrimination performance is better than that predicted from Weber's law. Specifically, we used signal detection theory in order to quantitatively compare our results, perceptual discrimination performance, with those of Mallery et al. (10). It is noteworthy that this approach is more general than that taken in previous neurophysiological studies, which have observed that inverse neural gain scales linearly with stimulus amplitude (14, 15). This so-called “Weber adaptation” has been proposed to be a neural correlate of Weber's law and is a form of contrast gain scaling (73). Theoretically, however, neural discrimination performance should depend on variability as well as gain. Indeed, our present results show that only taking into account gain would give an incorrect prediction as to behavioral performance. This is because the inverse gain scaled linearly with stimulus amplitude (Fig. 1E, *Inset*), which would incorrectly predict that neural discrimination thresholds increase linearly with stimulus amplitude. In contrast, only taking into account the amplitude dependence of neural variability (Fig. 1F) would instead predict discrimination thresholds that initially increase linearly and then saturate at higher stimulus amplitudes, which better corresponds with perceptual results (10). This

approach is more similar to that typically taken in psychophysical studies to measure the JND using the within-subject variability in the behavioral response (e.g., refs. 74 to 75). In this context, while neural discrimination thresholds are theoretically determined by both gain and variability, our results show that the change in slope observed for neural discrimination thresholds for vestibular thalamocortical neurons is primarily due to the fact that neural variability saturated at higher stimulus amplitudes, which better predicts improved behavioral discrimination performance. We note that this argument assumes that behavioral variability scales with neural variability. This assumption appears to be justified as a recent study has shown a positive correlation between neural and behavioral variability in the vestibular system (11).

We predict that a violation of Weber's law will also be seen for dynamic translations and will have a neural correlate similar to that reported here for rotations. The fact that vestibular thalamocortical neurons display similar nonlinear responses to dynamic rotations and translations supports our prediction (37, 40). To date, the only psychophysical study that investigated discrimination thresholds for dynamic translations focused on relatively low amplitudes (i.e., <1 G) because of mechanical limitations (76). Further studies exploring higher stimulation amplitudes found in natural self-motion stimuli (3 to 4 G) (26) are thus necessary to verify our prediction.

Our findings raise the fundamental question: Why is there a violation of Weber's law for self-motion perception in the first place? As previously stated, perceptual discrimination thresholds are lower than predicted from Weber's law for higher stimulus amplitudes, meaning that subjects actually performed better at discriminating between different amplitudes (10). It has been suggested that improved discrimination performance contributes to the vestibular system's ability to sense motion and maintain balance, even for more challenging (higher intensity) stimuli (10, 11). However, this then also leads to the follow-up question of whether there is a cost for this improvement. Theoretical studies have suggested that Weber's law is associated with optimized neural coding at the neural level (14, 15, 17–21). Accordingly, one could assume that psychophysical performance cannot be greater than that predicted from Weber's law. However, an assumption inherent to these theoretical studies is that neural variability did not depend on stimulus amplitude, which we show is not true for vestibular thalamocortical neurons. Therefore, to explain this apparent discrepancy, we hypothesize that stimulus amplitude-dependent neural variability plays a key role toward further optimizing the coding of natural self-motion stimuli whose amplitude varies over three orders of magnitude beyond what is achieved by Weber adaptation alone. Specifically, our results show that the fact that neural variability saturates at higher stimulus amplitudes improves neural discrimination performance, which is expected to improve coding of high amplitudes commonly observed during natural self-motion. Further studies using natural self-motion stimuli are needed to test this proposal.

Finally, we speculate that neural variability in other sensory systems depends on stimulus amplitude in a manner similar to that seen here for vestibular thalamocortical neurons, thus providing a neural correlate of improved perceptual discrimination performance for higher stimulus amplitudes. Studies exploring larger ranges of stimulus amplitudes found under natural conditions are needed to test this prediction. While Weber adaptation has been observed in other systems (14, 15), these studies did not consider the effects of neural variability. Hence, we further predict that the violations of Weber's law seen across sensory modalities reflect optimized coding by sensory neurons when variability is taken into account, which will ultimately lead to a comprehensive rethinking of how optimized coding gives rise to perception in general.

## Materials and Methods

**Ethics.** All experimental procedures were approved by the McGill University and Johns Hopkins University Animal Care Committees. Procedures were in compliance with the guidelines of the Canadian Council on Animal Care.

**Surgical Procedures.** Two male and one female rhesus monkeys (*M. Mulatta*) were prepared for acute extracellular recordings using aseptic, MRI-guided surgical techniques, as described previously (40). Surgical levels of isoflurane (0.8 to 1.5%) were maintained during surgery, during which the animals were implanted with a custom-made medical grade titanium head post for restraining the head and a recording chamber that was placed based on the coregistration of a computed tomography (CT) scan, an MRI scan, and the rhesus brain atlas in Brainsight (Brainsight 2 Vet, Rogue Research) to provide access to VPL. VPL access position was confirmed postsurgery by the coregistration of a second CT scan with a recording electrode maintained in the center of the recording chamber. The implant was chronically fastened to the skull with titanium screws and Simplex P bone cement (Stryker Orthopedics). An 18-mm eye coil (three loops of Teflon-insulated stainless-steel wire) was also implanted behind the conjunctiva of one eye in each monkey (77). Finally, buprenorphine (0.01 mg/kg, IM) and cefazolin (25 mg/kg) were administered as postoperative analgesia and antibiotic, respectively. Animals recovered for at least 2 wk before recordings began.

**Data Acquisition.** Throughout recordings, head-restrained monkeys were seated in a primate chair that was mounted on a motion platform rotating about the vertical axis (i.e., yaw rotation) within a dark room. Eye movements were measured using the magnetic search coil technique (77). Turntable velocity was controlled by REX, a QNX-based, real-time data acquisition system (78), and measured using an angular rate sensor (Watson Industries, Inc.). All behavioral signals were low pass filtered at 250 Hz and acquired at 1-kHz sampling frequency. The VPL was located relative to the lateral geniculate nucleus, which was recognizable because of the presence of individual neurons that responded to either the onset or offset of a light flashed while lowering the electrode during early recordings (79). Each neuron included in the present report demonstrated robust firing rate modulation during sinusoidal, whole-body rotations and were not sensitive to eye movements during saccades or smooth pursuit (37, 80). Furthermore, we ensured that neurons did not respond to the visual stimulation caused by small spots of light presented in the visual field (79). Extracellular, single-unit activity was recorded using enamel-insulated tungsten microelectrodes (2 to 10 M $\Omega$  impedance, Frederick Haer), band pass filtered from 300 Hz to 3 kHz, and sampled at 30 kHz. Both neural and behavioral data were acquired through the Cerebus Neural Signal Processor (Blackrock Microsystems).

**Stimulation.** Neurons were initially identified on the basis of their response to passive rotations in the dark in the absence of visual stimulation (i.e., whole-body rotations). The same vestibular stimuli were then applied with the lights on to confirm that there was no change in mean firing rate or gain due to responses to visual stimulation. Our stimuli consisted of sinusoidal, whole-body rotations along the yaw axis with frequencies 0.5, 1, 2, 3, 4, 5, 8, and 17 Hz whose amplitude increased between 0 and 100 deg/s within a duration of 100 s (ramp up) and then back to 0 deg/s within a duration of 100 s (ramp down). Overall, variations in neural activity were similar during both the ramp-up and ramp-down portions of the stimulus. Results were thus averaged between both portions.

**Data Analysis.** Neural data were imported into MATLAB (The MathWorks) for sorting as well as for all offline analysis. For each neuron, spike times were converted into a binary sequence sampled at 1 kHz. Specifically, time was discretized into bins of 1 ms length, and the content of each bin was set to 1,000 if one spike occurred within and to 0 otherwise. Note that, as the bin width is less than the neuron's absolute refractory period, at most, one spike could occur during any given bin.

The time-dependent firing rate was obtained by low-pass filtering the binary sequence with a Kaiser filter whose cutoff was 0.5 Hz above the stimulus frequency (81). The time-dependent firing rate was then aligned to be in phase with the head velocity stimulus using the cross-correlation function (36). The head velocity was discretized into bins of 2 deg/s, and we verified that the firing rate distributions for each bin were normal using a Lilliefors test ( $P > 0.08$  in all cases). Discrimination thresholds were defined as the minimum change in head velocity from a given amplitude for which the firing rate distribution could be reliably discriminated. Specifically, discriminability between firing rate distributions was quantified using  $d'$  (42):

$$d' = \frac{|\mu_1 - \mu_0|}{\sqrt{(\sigma_1^2 + \sigma_0^2)/2}} \quad [1]$$

where  $\mu_0$  and  $\mu_1$  are means of the distributions and  $\sigma_0^2$  and  $\sigma_1^2$  their variances. Now, assuming that  $\sigma_0^2 = \sigma_1^2 = \sigma^2$  distributions are discriminable, if  $d' = 1.16$  (82), and rearranging Eq. 1 gives the following:

$$\Delta\mu = 1.16 \sigma, \quad [2]$$

where  $\Delta\mu$  is, then the minimum change in firing rate that gives rise to distributions with SD  $\sigma$  that are discriminable from one another. Now, changes in firing rate are related to changes in head velocity  $\Delta v$  by the gain  $G$  for a linear system, which gives the following:

$$\Delta v = 1.16 \frac{\sigma}{G} \quad [3]$$

where  $\Delta v$  is the minimum change in head velocity that gives rises to a change in firing rate that can be discriminated from random fluctuations and thus corresponds to the discrimination threshold. In practice, we used a pedestal (i.e., reference) head velocity value of zero. We note that discrimination thresholds are actually independent of the pedestal value chosen because the firing rate is a linear function of the instantaneous head velocity. Furthermore, we used a value of  $d' = 1.16$ , as this corresponds to a probability of correct detection of 79.4%, which is the same value as that used in a previous psychophysical study (10), which allows for better comparison between results. We note that both the variability  $\sigma$  and the gain  $G$  can depend on stimulus amplitude if there are nonlinearities present in the neural response. We note that there can be large differences in threshold values when using different methodologies to obtain the firing rate (57). However, threshold values will then be the same up to a scaling factor, and this will not affect the qualitative nature of our results.

Weber's law states that the JND divided by the stimulation amplitude should be constant (1). Thus, neural discrimination thresholds should increase linearly with stimulus amplitude and deviations from linearity were quantified as  $1-R^2$ , where  $R^2$  is the goodness of fit from a linear least-squares fit to the discrimination threshold as a function of the stimulus amplitude. Discrimination thresholds were computed from Eq. 3 for time windows of 2 s that were moved over time in increments of 1 ms. The firing rate during each time window was aligned to be in phase with the head

velocity stimulus by computing the cross-correlation and finding the position of the peak, as done previously (36). The gain was computed from the slope of the best-fit straight line when plotting the firing rate aligned with the head velocity stimulus. Variability was computed as the SD of the firing rate distribution. In practice, gain and variability values were averaged between the ramp-up and ramp-down portions of the stimulus and were low pass filtered (first-order Butterworth, 0.5 Hz cutoff) before taking their ratio to compute the discrimination threshold. Discrimination thresholds were then plotted as a function of the mean stimulus amplitude during each time window.

We combined neural activities, assuming that each neuron acts as an individual channel of information (i.e., response variabilities are assumed to be independent of one another). In which case, the variability for  $n$  neurons is given by the following (83):

$$\sigma_n = \sqrt{n} \sigma, \quad [4]$$

where  $\sigma = \sigma_1$  is the average variability for a single neuron. The gain for  $n$  neurons is given by the following:

$$G_n = n G, \quad [5]$$

where  $G = G_1$  is the average gain for a single neuron. We note that this is because the change in the population firing rate is then  $n$  times the change in the single-neuron firing rate. The discrimination threshold is then given by the following:

$$\Delta v_n = \frac{\Delta v}{\sqrt{n}} \quad [6]$$

where  $\Delta v = \Delta v_1$  is the average discrimination threshold of a single neuron. We used Eq. 6 to compute discrimination thresholds as a function of population size  $n$ .

**Data Availability.** All study data are included in the article and/or *SI Appendix*.

**ACKNOWLEDGMENTS.** We thank S. Nuara and S. Frey for technical support as well as G. McAllister and H. Hooshangnejad for help with gathering data. This research was supported by project grant 162285 from the Canadian Institutes of Health Research (J.C., K.E.C., and M.J.C.) as well as grants R01-DC002390 and R01-DC018061 from the NIH (K.E.C.).

1. E. H. Weber, *De Pulsu, Resorptione, Auditu Et Tactu. Annotationes Anatomicae Et Physiologicae* (Lipsiae [Leipzig] C. F. Koehler, 1834).
2. G. Fechner, *Elemente der Psychophysik* (Breitkopf & Härtel, Leipzig, 1860).
3. E. M. Brannon, M. E. Libertus, W. H. Meck, M. G. Woldorff, Electrophysiological measures of time processing in infant and adult brains: Weber's law holds. *J. Cogn. Neurosci.* **20**, 193–203 (2008).
4. D. R. J. Laming, *Sensory Analysis* (Academic Press, London, 1986).
5. G. A. Gescheider, *Psychophysics: The Fundamentals* (Lawrence Erlbaum Associates, Mahwah, NJ, 2013).
6. J. C. Baird, *Sensation and Judgement* (Lawrence Erlbaum Associates, Mahwah, NJ, 1997).
7. C. W. Doble, J.-C. Falmagne, B. G. Berg, Recasting (the near-miss to) Weber's law. *Psychol. Rev.* **110**, 365–375 (2003).
8. W. J. McGill, J. P. Goldberg, Pure-tone intensity discrimination and energy detection. *J. Acoust. Soc. Am.* **44**, 576–581 (1968).
9. T. Augustin, T. Roscher, Empirical evaluation of the near-miss-to-Weber's law: A visual discrimination experiment. *Psychol. Sci. Q.* **50**, 469–488 (2008).
10. R. M. Mallery, O. U. Olomu, R. M. Uchanski, V. A. Militchin, T. E. Hullar, Human discrimination of rotational velocities. *Exp. Brain Res.* **204**, 11–20 (2010).
11. S. Nouri, F. Karmali, Variability in the vestibulo-ocular reflex and vestibular perception. *Neuroscience* **393**, 350–365 (2018).
12. A. Nesti, K. A. Beykirch, P. Pretto, H. H. Bühlhoff, Human discrimination of head-centred visual-inertial yaw rotations. *Exp. Brain Res.* **233**, 3553–3564 (2015).
13. T. Augustin, The parameters in the near-miss-to-Weber's law. *J. Math. Psychol.* **52**, 37–47 (2008).
14. S. Gorur-Shandilya, M. Demir, J. Long, D. A. Clark, T. Emonet, Olfactory receptor neurons use gain control and complementary kinetics to encode intermittent odorant stimuli. *eLife* **6**, e27670 (2017).
15. K. Donner, D. R. Copenhagen, T. Reuter, Weber and noise adaptation in the retina of the toad *Bufo marinus*. *J. Gen. Physiol.* **95**, 733–753 (1990).
16. H. B. Barlow, Optic nerve impulses and Weber's law. *Cold Spring Harb. Symp. Quant. Biol.* **30**, 539–546 (1965).
17. B. Wark, B. N. Lundstrom, A. Fairhall, Sensory adaptation. *Curr. Opin. Neurobiol.* **17**, 423–429 (2007).
18. J. L. Pardo-Vazquez et al., The mechanistic foundation of Weber's law. *Nat. Neurosci.* **22**, 1493–1502 (2019).
19. J. M. Zanker, Does motion perception follow Weber's law? *Perception* **24**, 363–372 (1995).
20. T. O. Sharpee et al., Adaptive filtering enhances information transmission in visual cortex. *Nature* **439**, 936–942 (2006).
21. T. O. Sharpee, A. J. Calhoun, S. H. Chalasani, Information theory of adaptation in neurons, behavior, and mood. *Curr. Opin. Neurobiol.* **25**, 47–53 (2014).
22. J. M. Goldberg et al., *The Vestibular System: A Sixth Sense* (Oxford University Press, New York, 2012).
23. E. G. Walsh, The perception of rhythmically repeated linear motion in the vertical plane. *Q. J. Exp. Physiol. Cogn. Med. Sci.* **49**, 58–65 (1964).
24. T. Okada, E. Grunfeld, J. Shallo-Hoffmann, A. M. Bronstein, Vestibular perception of angular velocity in normal subjects and in patients with congenital nystagmus. *Brain* **122**, 1293–1303 (1999).
25. Y. Valko, R. F. Lewis, A. J. Priesol, D. M. Merfeld, Vestibular labyrinth contributions to human whole-body motion discrimination. *J. Neurosci.* **32**, 13537–13542 (2012).
26. J. Carriot, M. Jamali, M. J. Chacron, K. E. Cullen, Statistics of the vestibular input experienced during natural self-motion: Implications for neural processing. *J. Neurosci.* **34**, 8347–8357 (2014).
27. K. E. Cullen, The vestibular system: Multimodal integration and encoding of self-motion for motor control. *Trends Neurosci.* **35**, 185–196 (2012).
28. V. Marlinski, R. A. McCrea, Self-motion signals in vestibular nuclei neurons projecting to the thalamus in the alert squirrel monkey. *J. Neurophysiol.* **101**, 1730–1741 (2009).
29. U. Büttner, W. Lang, The vestibulocortical pathway: Neurophysiological and anatomical studies in the monkey. *Prog. Brain Res.* **50**, 581–588 (1979).
30. W. O. Guldin, O. J. Grüsser, Is there a vestibular cortex? *Trends Neurosci.* **21**, 254–259 (1998).
31. R. Gonçalves et al., Clinical and topographic magnetic resonance imaging characteristics of suspected thalamic infarcts in 16 dogs. *Vet. J.* **188**, 39–43 (2011).
32. B. J. Clark, R. E. Harvey, Do the anterior and lateral thalamic nuclei make distinct contributions to spatial representation and memory? *Neurobiol. Learn. Mem.* **133**, 69–78 (2016).
33. S. G. Sadeghi, M. J. Chacron, M. C. Taylor, K. E. Cullen, Neural variability, detection thresholds, and information transmission in the vestibular system. *J. Neurosci.* **27**, 771–781 (2007).
34. S. G. Sadeghi, L. B. Minor, K. E. Cullen, Response of vestibular-nerve afferents to active and passive rotations under normal conditions and after unilateral labyrinthectomy. *J. Neurophysiol.* **97**, 1503–1514 (2007).



35. A. D. Schneider, M. Jamali, J. Carriot, M. J. Chacron, K. E. Cullen, The increased sensitivity of irregular peripheral canal and otolith vestibular afferents optimizes their encoding of natural stimuli. *J. Neurosci.* **35**, 5522–5536 (2015).
36. C. Massot, M. J. Chacron, K. E. Cullen, Information transmission and detection thresholds in the vestibular nuclei: Single neurons vs. population encoding. *J. Neurophysiol.* **105**, 1798–1814 (2011).
37. V. Marlinski, R. A. McCrea, Activity of ventroposterior thalamus neurons during rotation and translation in the horizontal plane in the alert squirrel monkey. *J. Neurophysiol.* **99**, 2533–2545 (2008).
38. H. Meng, D. E. Angelaki, Responses of ventral posterior thalamus neurons to three-dimensional vestibular and optic flow stimulation. *J. Neurophysiol.* **103**, 817–826 (2010).
39. H. Meng, P. J. May, J. D. Dickman, D. E. Angelaki, Vestibular signals in primate thalamus: Properties and origins. *J. Neurosci.* **27**, 13590–13602 (2007).
40. A. Dale, K. E. Cullen, The ventral posterior lateral thalamus preferentially encodes externally applied versus active movement: Implications for self-motion perception. *Cereb. Cortex* **29**, 305–318 (2019).
41. L. Deecke, D. W. Schwarz, J. M. Fredrickson, Vestibular responses in the rhesus monkey ventroposterior thalamus. II. Vestibulo-proprioceptive convergence at thalamic neurons. *Exp. Brain Res.* **30**, 219–232 (1977).
42. D. M. Green, J. A. Swets, *Signal Detection Theory and Psychophysics* (John Wiley & Sons, New York, 1966).
43. N. C. Rabinowitz, B. D. Willmore, J. W. H. Schnupp, A. J. King, Contrast gain control in auditory cortex. *Neuron* **70**, 1178–1191 (2011).
44. R. B. Stein, E. R. Gossen, K. E. Jones, Neuronal variability: Noise or part of the signal? *Nat. Rev. Neurosci.* **6**, 389–397 (2005).
45. M. D. McDonnell, L. M. Ward, The benefits of noise in neural systems: Bridging theory and experiment. *Nat. Rev. Neurosci.* **12**, 415–426 (2011).
46. M. M. Churchland *et al.*, Stimulus onset quenches neural variability: A widespread cortical phenomenon. *Nat. Neurosci.* **13**, 369–378 (2010).
47. A. Ponce-Alvarez, A. Thiele, T. D. Albright, G. R. Stoner, G. Deco, Stimulus-dependent variability and noise correlations in cortical MT neurons. *Proc. Natl. Acad. Sci. U.S.A.* **110**, 13162–13167 (2013).
48. G. Hennequin, Y. Ahmadian, D. B. Rubin, M. Lengyel, K. D. Miller, The dynamical regime of sensory cortex: Stable dynamics around a single stimulus-tuned attractor account for patterns of noise variability. *Neuron* **98**, 846–860.e5 (2018).
49. A. Litwin-Kumar, B. Doiron, Slow dynamics and high variability in balanced cortical networks with clustered connections. *Nat. Neurosci.* **15**, 1498–1505 (2012).
50. A. Renart *et al.*, The asynchronous state in cortical circuits. *Science* **327**, 587–590 (2010).
51. T. Tetzlaff, M. Helias, G. T. Einevoll, M. Diesmann, Decorrelation of neural-network activity by inhibitory feedback. *PLoS Comput. Biol.* **8**, e1002596 (2012).
52. G. Hennequin, T. P. Vogels, W. Gerstner, Optimal control of transient dynamics in balanced networks supports generation of complex movements. *Neuron* **82**, 1394–1406 (2014).
53. B. K. Murphy, K. D. Miller, Balanced amplification: A new mechanism of selective amplification of neural activity patterns. *Neuron* **61**, 635–648 (2009). Correction in: *Neuron* **89**, 235 (2016).
54. M. Jamali, J. Carriot, M. J. Chacron, K. E. Cullen, Coding strategies in the otolith system differ for translational head motion vs. static orientation relative to gravity. *eLife* **8**, e45573 (2019).
55. S. Akbarian, O. J. Grüsser, W. O. Guldin, Corticofugal connections between the cerebral cortex and brainstem vestibular nuclei in the macaque monkey. *J. Comp. Neurol.* **339**, 421–437 (1994).
56. C. Lopez, O. Blanke, The thalamocortical vestibular system in animals and humans. *Brain Res. Brain Res. Rev.* **67**, 119–146 (2011).
57. M. Jamali, J. Carriot, M. J. Chacron, K. E. Cullen, Strong correlations between sensitivity and variability give rise to constant discrimination thresholds across the otolith afferent population. *J. Neurosci.* **33**, 11302–11313 (2013).
58. X.-J. Yu, J. D. Dickman, D. E. Angelaki, Detection thresholds of macaque otolith afferents. *J. Neurosci.* **32**, 8306–8316 (2012).
59. B. Clark, Thresholds for the perception of angular acceleration in man. *Aerosp. Med.* **38**, 443–450 (1967).
60. F. Guedry Jr, “Psychophysics of vestibular sensation” in *Handbook of Sensory Physiology*, H. H. Kornhuber, Ed. (Springer, New York, 1974), pp. 3–154.
61. L. Grabherr, K. Nicoucar, F. W. Mast, D. M. Merfeld, Vestibular thresholds for yaw rotation about an earth-vertical axis as a function of frequency. *Exp. Brain Res.* **186**, 677–681 (2008).
62. E. G. Walsh, Role of the vestibular apparatus in the perception of motion on a parallel swing. *J. Physiol.* **155**, 506–513 (1961).
63. E. G. Walsh, The perception of rhythmically repeated linear motion in the horizontal plane. *Br. J. Psychol.* **53**, 439–445 (1962).
64. L. R. Young, J. L. Meiry, A revised dynamic otolith model. *Aerosp. Med.* **39**, 606–608 (1968).
65. A. J. Benson, M. B. Spencer, J. R. Stott, Thresholds for the detection of the direction of whole-body, linear movement in the horizontal plane. *Aviat. Space Environ. Med.* **57**, 1088–1096 (1986).
66. G. M. Jones, L. R. Young, Subjective detection of vertical acceleration: A velocity-dependent response? *Acta Otolaryngol.* **85**, 45–53 (1978).
67. J. Carriot, M. Jamali, M. J. Chacron, K. E. Cullen, The statistics of the vestibular input experienced during natural self-motion differ between rodents and primates. *J. Physiol.* **595**, 2751–2766 (2017).
68. C. Pozzorini, R. Naud, S. Mensi, W. Gerstner, Temporal whitening by power-law adaptation in neocortical neurons. *Nat. Neurosci.* **16**, 942–948 (2013).
69. Y. Dan, J. J. Atick, R. C. Reid, Efficient coding of natural scenes in the lateral geniculate nucleus: Experimental test of a computational theory. *J. Neurosci.* **16**, 3351–3362 (1996).
70. C. G. Huang, Z. D. Zhang, M. J. Chacron, Temporal decorrelation by SK channels enables efficient neural coding and perception of natural stimuli. *Nat. Commun.* **7**, 11353 (2016).
71. D. E. Mitchell, A. Kwan, J. Carriot, M. J. Chacron, K. E. Cullen, Neuronal variability and tuning are balanced to optimize naturalistic self-motion coding in primate vestibular pathways. *eLife* **7**, e43019 (2018).
72. D. M. Merfeld, L. H. Zupan, Neural processing of gravito-inertial cues in humans. III. Modeling tilt and translation responses. *J. Neurophysiol.* **87**, 819–833 (2002).
73. M. Carandini, D. J. Heeger, Normalization as a canonical neural computation. *Nat. Rev. Neurosci.* **13**, 51–62 (2011). Correction in: *Nat. Rev. Neurosci.* **14**, 152 (2013).
74. T. Ganel, E. Chajut, D. Algom, Visual coding for action violates fundamental psychophysical principles. *Curr. Biol.* **18**, R599–R601 (2008).
75. G. B. Evans, E. Howarth, The effect of grip-tension on tactile-kinaesthetic judgement of width. *Q. J. Exp. Psychol.* **18**, 275–277 (1966).
76. A. R. Naseri, P. R. Grant, Human discrimination of translational accelerations. *Exp. Brain Res.* **218**, 455–464 (2012).
77. A. F. Fuchs, D. A. Robinson, A method for measuring horizontal and vertical eye movement chronically in the monkey. *J. Appl. Physiol.* **21**, 1068–1070 (1966).
78. A. V. Hayes, B. J. Richmond, L. M. Optican, “A UNIX-based multiple process system for real-time data acquisition and control” in WESCON Conf. Proc. (1982). <https://www.osti.gov/biblio/5213621>. Accessed 26 August 2021.
79. R. T. Marrocco, Sustained and transient cells in monkey lateral geniculate nucleus: Conduction velocities and response properties. *J. Neurophysiol.* **39**, 340–353 (1976).
80. J. E. Roy, K. E. Cullen, Selective processing of vestibular reafference during self-generated head motion. *J. Neurosci.* **21**, 2131–2142 (2001).
81. S. Cherif, K. E. Cullen, H. L. Galiana, An improved method for the estimation of firing rate dynamics using an optimal digital filter. *J. Neurosci. Methods* **173**, 165–181 (2008).
82. H. P. Snippe, J. J. Koenderink, Discrimination thresholds for channel-coded systems. *Biol. Cybern.* **66**, 543–551 (1992).
83. E. Zohary, M. N. Shadlen, W. T. Newsome, Correlated neuronal discharge rate and its implications for psychophysical performance. *Nature* **370**, 140–143 (1994).